Available online at www.sciencedirect.com
ScienceDirect
Biochimica et Biophysica Acta 1773 (2007) 513–520
Biochimica et Biophysica Acta BBA
www.elsevier.com/locate/bbamcr

Visualization of CD146 dimerization and its regulation in living cells

Pengcheng Bu [a,b], Jie Zhuang [a,b], Jing Feng [a], Dongling Yang [a], Xun Shen [a], Xiyun Yan [a,*]

[a] National Laboratory of Biomacromolecules, Institute of Biophysics, Chinese Academy of Sciences, 15 Datun Road, Beijing 100101, China
[b] Graduate School, Chinese Academy of Sciences, Beijing 100039, China

Received 25 September 2006; received in revised form 30 December 2006; accepted 19 January 2007
Available online 27 January 2007

Abstract

Our previous study showed that the adhesion molecule CD146 as a biomarker is over-expressed on activated endothelium during angiogenesis, which was induced by tumor conditional medium and inhibited by anti-CD146 monoclonal antibody (mAb AA98). However, the CD146 molecular organization on the cells is unknown. Here, using immunoprecipitation, we found that the dimerization of CD146 occurs in both normal and tumor cells. However, the dimer/monomer ratio was higher in tumor cells than in normal cells. Moreover, we found that CD146 dimerization was up-regulated by tumor conditional medium through the NF-kappa B pathway and down-regulated by mAb AA98. To further confirm that CD146 dimerization occurs in living cells, we used fluorescence resonance energy transfer (FRET) with melanoma Mel888 cells co-expressing CFP/YFP-tagged CD146 fusion proteins. By acceptor photobleaching, we observed a strong FRET signal produced by these two fluorescence-tagged proteins. The FRET efficiency reached 20.1%. Our data provide the first evidence that CD146 dimerization occurs in living cells and is regulated within the tumor microenvironment, implying that dimerization of CD146 may be associated with malignancy.

Keywords: CD146; Dimerization; FRET; NF-kappa B

1. Introduction

Adhesion molecule CD146 (100–130 kDa) belongs to the immunoglobulin superfamily. The sequence of CD146 is highly homologous to a number of cell adhesion molecules such as NCAM [1] and contains a V-V-C2-C2-C2 Ig-like extracellular domain, a single membrane-spanning, and a short cytoplasmic domain. The CD146 molecule was originally identified as a biomarker for melanoma [2–4] and is involved in tumor progression and metastasis. It has been shown that the enforced expression of CD146 in melanoma cells increases melanoma growth and metastasis [5], whereas the decrease of CD146 expression results in reduced tumorigenicity [6]. Mills et al. have reported that anti-CD146 antibody significantly inhibits tumor growth and metastasis of human melanoma [7]. These data indicate that CD146 plays an important role in promoting melanoma progression.

Another important set of data has identified CD146 as a marker on angiogenic vascular endothelium [8,9] and a structural component of interendothelial junctions [10]. A number of studies have addressed the biological function of CD146 in blood vessels. For instance, Chan et al. reported that the suppression of CD146 protein expression by antisense oligonucleotides results in poor vascular development in zebrafish [11]. Our results showed that the CD146 molecule is over-expressed on the activated endothelium of many different tumors, and this expression is induced by tumor conditional medium, resulting in increased cell adhesion, migration and angiogenesis. Conversely, the induced endothelial cell activities and angiogenesis could be inhibited by anti-CD146 monoclonal antibody (mAb AA98) [8]. In addition, we and others found that CD146 plays an important role in cell migration and invasion based on the observation that CD146 is predominantly expressed on invasive intermediate trophoblasts rather than non-invasive cytotrophoblasts [12–14]. Our finding that CD146 expression was absence on the placenta of pre-eclampsia [12] also supports the idea that the CD146 is a critical molecule in embryo implantation and pregnancy disorder.

* Corresponding author. Tel.: +86 10 64888583; fax: +86 10 64888584.
E-mail address: yanxy@sun5.ibp.ac.cn (X. Yan).

0167-4889/$ - see front matter © 2007 Elsevier B.V. All rights reserved.
doi:10.1016/j.bbamcr.2007.01.009

Although the CD146 ligand has not been identified, the engagement of CD146 with anti-CD146 antibodies has profound effects on cellular functions. It has been shown that CD146 mediates Ca^{2+}-independent homotypic and heterotypic cell–cell interaction on cultured endothelial cells and is involved in control of intercellular permeability [15]. Additional studies indicated that CD146 induces the association of tyrosine kinase $p59^{fyn}$ with the cytoplasmic tail of CD146 and the phosphorylation of $p125^{FAK}$ and paxillin in human umbilical vein endothelial cells [16]. These findings indicate that CD146 does not act as merely "molecule glue", but is actively involved in outside-in signaling and in the control of cell–cell contact. However, the underlying mechanism remains unclear.

Given that many receptors and adhesion molecules are functional as dimers or oligomers when interacting with extracellular factors [17,18], which is a key event in signaling transduction [19], we hypothesized that the oligomerization of CD146 might occur in cells and be associated with cell activity. To test this, we performed FRET and immunoprecipitation to study the molecular organization of CD146 in living cells. Our results provide the first evidence that CD146 dimerization occurs in living cells, and is down-regulated by mAb AA98 and up-regulated by tumor conditional medium through the NF-kappa B pathway.

2. Materials and methods

2.1. Cell lines and antibodies

Human melanoma cell A375 and normal vascular endothelial cell ECV304, both of which are natively CD146-expressing cells, were obtained from American Type Culture Collection (Rockville). Mel888 is a human melanoma cell line, which does not express CD146. CD146-positive Mel888 is the Mel888 cell transfected with CD146, which was kindly provided by Dr. Judith P. Johnson (University of Munich, Germany). All the cells were cultured in Dulbecco modified Eagle medium (DMEM) containing 10% fetal-calf serum (FCS).

Antibodies used in this study were anti-NF-kappa B (p65), anti-IκBα, anti-β-actin purchased from Santa Cruz, horseradish peroxidase (HRP)-conjugated anti-mouse or anti-rabbit IgG purchased from Pierce, and rabbit anti-CD146 antibody and mAb AA98 produced in our lab.

2.2. Preparation of conditional medium

Melanoma cells A375 were cultured with DMEM in a 10 cm culture plate. After 24-h culture, the supernatant from the culture was collected and used as conditional medium (named as A375-CM).

2.3. Construction of tagged CD146

The cDNA encoding full length of human CD146 with its signal peptide was amplified by PCR using pUC18-CD146 plasmid as template (kindly provided by Dr. Judith P. Johnson, University of Munich, Germany). The primers used were 5′-cgggaattcatggggcttcccaggctg-3′ (*Eco*RI underlined) and 5′-cccggatccatgcctcagatcgatgtatttc-3′ (*Bam*HI underlined). The PCR products of CD146 gene were then inserted into the vector of pEyFP-N1 and pEcFP-N1 (Clontech), producing $CD146_{YFP}$ and $CD146_{CFP}$ constructs.

2.4. Fluorescence microscopy

Mel888 cells were co-transfected with $CD146_{YFP}$ and $CD146_{CFP}$ constructs. After 48 h culture, these transfected cells were fixed in 4% cold formaldehyde/PBS for 4 min at room temperature, followed by observation under a confocal laser scanning microscope (FV500, Olympus). For mAb AA98 staining, these cells were continuously incubated overnight at 4 °C with mAb AA98, then with biotin labeled anti-mouse IgG for 1 h, and finally with avidin-conjugated cychrome (BD Pharmingen) for 1 h. After carefully washing with PBS, the cells were examined under a fluorescence microscope with excitation at 510 nm and emission at 630 nm.

For detection of the regulation of NF-kappa B activity, the endothelial cells ECV304 were treated for 30 min with an inhibitor of NF-kappa B, BAY 11-7082 (10 nM, Calbiochem) and then cultured with A375-CM for 2 days. The treated cells were fixed in 4% cold formaldehyde/PBS for 4 min, permeabilized with 0.2% Triton X-100, and incubated for 30 min in 5% goat serum/PBS. After reaction with anti-NF-kappa B (p65) overnight at 4 °C, and then incubation with FITC-conjugated anti-mouse IgG antibody for another 1 h, the cells were examined under a confocal laser scanning microscope.

2.5. FRET measurements

To generate cells co-expressing $CD146_{YFP}/CD146_{CFP}$ cells, the Mel888 cells were co-transfected with 2 μg of the $CD146_{YFP}/CD146_{CFP}$ constructs mixed with Lipofectamine 2000 according to the instructions of the manufacturer (Invitrogen). After 48 h of culture, these cells were washed with cold PBS and fixed in cold 4% formaldehyde/PBS for 4 min at room temperature. Image processing was performed under the confocal laser scanning microscope. Filters used for observing $CD146_{CFP}$ allowed excitation at 458 nm and emission at 465–495 nm; for $CD146_{YFP}$ excitation at 515 nm and emission

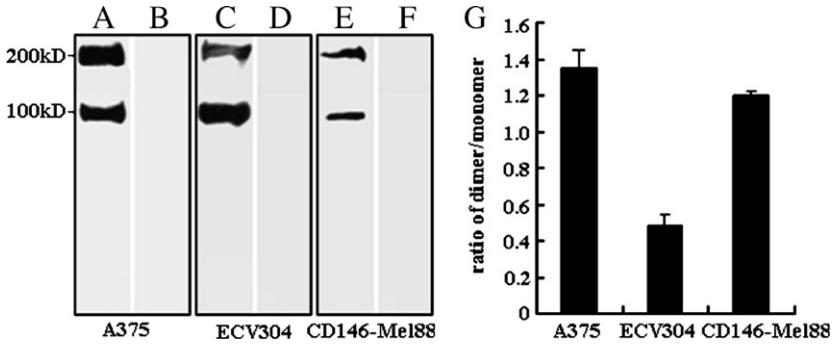

Fig. 1. CD146 dimerization is detected in various cells. Cell lysates from melanoma A375, vascular endothelial ECV304 and CD146-forced expressing Mel888 CD146-Mel888 were immunoprecipitated with anti-CD146 mAb AA98, followed by Western blotting with rabbit anti-CD146 antibody. The CD146 dimer (200 kDa) and monomer (100 kDa) were specifically recognized by the two antibodies (A, C, and E). No cross-reaction with other proteins was detected by secondary anti-rabbit IgG antibodies (B, D, and F). The ratio of the CD146 dimer and monomer were qualified by densitometry using the data from three independent experiments (G).

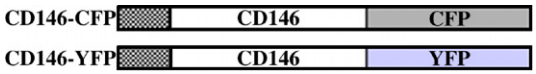

Fig. 2. Schematic representation of fluorescence tagged CD146 constructs. The $CD146_{CFP}$ and $CD146_{YFP}$ were constructed by fusing CFP or YFP at the C-terminus of CD146. The N-terminus of CD146 contains a signal peptide.

at 565–595 nm was used; for FRET of $CD146_{YFP}$ and $CD146_{CFP}$ excitation was at 458 nm and emission at 565–595 nm.

Acceptor photobleaching was performed to test the specificity of FRET. The $CD146_{YFP}$ as acceptor fluorophore was selectively photobleached for 2 min at 515 nm (meanwhile the 458 nm scanning window was set to zero for prevent any CFP photobleaching), and the increase in fluorescence intensity of the donor $CD146_{CFP}$ was measured. The FRET efficiency E is given by: $E=1-(F_{da}/F_d)$, where F_{da} is the intensity of donor fluorescence when both donor and acceptor are present, and F_d is the donor fluorescence intensity after the acceptor was photobleached.

2.6. Immunoprecipitation

The cells of A375, ECV304 and CD146-positive Mel888 were respectively lysed in a culture dish by adding 0.6 mL ice-cold lysis buffer A (150 mM NaCl, 1 mM EDTA, 50 mM Tris, pH 8.0, 10% glycerol, 1% Triton X-100, 1 mM phenylmethylsulfonyl fluoride, and 25 μg/mL aprotinin). The supernatants were collected by centrifugation at 12,000×*g* at 4 °C for 10 min and then pre-cleaned with protein A-Sepharose (Sigma) to remove the protein A-bound proteins. The total amount of proteins in the pre-cleaned supernatants was measured by Bradford kit (Bio-Rad). Each sample containing total protein 3.2 mg was immunoprecipitated with either mAb AA98 or control mIgG at 4 °C for 2 h, followed by incubation with protein A-Sepharose for 1 h. Immunoprecipitates were washed twice with the lysis buffer and then boiled for 5 min in loading buffer.

2.7. Preparation of cytoplasmic and nuclear extracts

For analysis of NF-kappa B activation in the cells, ECV304 cells were treated with an inhibitor of NF-kappa B, BAY 11-7082 (10 nM) for 30 min, and then co-cultured with A375-CM for 2 days. After that, the cytoplasmic and nuclear extracts of the ECV304 cells were prepared. Briefly, the cells were washed twice and scraped into 1.0 mL of ice-cold PBS. After centrifugation at 3000×*g* at 4 °C for 5 min, the cell pellet was lysed in 60 μL lysis buffer B (10 mM Tris, pH 8.0, 1.5 mM $MgCl_2$, 1 mM 1, 4-Dithiothreitol (DTT), 0.1% NP-40, 1 mM phenylmethylsulfonyl fluoride and 25 μg/mL aprotinin) and then incubated on ice for 15 min followed by centrifugation at 12,000×*g* at 4 °C for 15 min. The supernatants (cytoplasmic fraction) were stored at 4 °C and the pellets containing nuclei were suspended in 60 μL buffer C (10 mM Tris, pH 8.0, 50 mM KCl, 100 mM NaCl, 1 mM phenylmethylsulfonyl fluoride and 25 μg/mL aprotinin) at 4 °C for 30 min. After centrifuged at 12,000×*g* at 4 °C for 15 min, the supernatants were saved as nuclear extracts and boiled for 5 min in loading buffer.

2.8. Western blotting

The sample containing 25 μg proteins from the cytoplasmic fraction and containing 20 μg proteins from the nuclear extract were loaded into 8% SDS-PAGE and transferred onto a Hybond membrane (Amersham). The membranes were blocked 1 h with 5% milk/PBS, incubated for 2 h with the primary antibodies anti-NF-kappa B (p65), anti-IκBα, anti-β-actin (Santa Cruz) or rabbit anti-CD146. Then the membranes were probed with HRP-conjugated anti-mouse or anti-rabbit IgG (Pierce), and detected by enhanced chemiluminescence (Pierce).

3. Results

3.1. Detection of CD146 dimerization in various cell lysates

Using immunoprecipitating with mAb AA98 and Western blotting with anti-CD146 rabbit polyclonal antibodies, we observed two bands at 100-kDa and 200-kDa in the immunoprecipitates of various cell lyses, including melanoma A375, vascular endothelial ECV304, and CD146-forced expressing Mel888 cells (Fig. 1A, C, E). The 100-kDa band

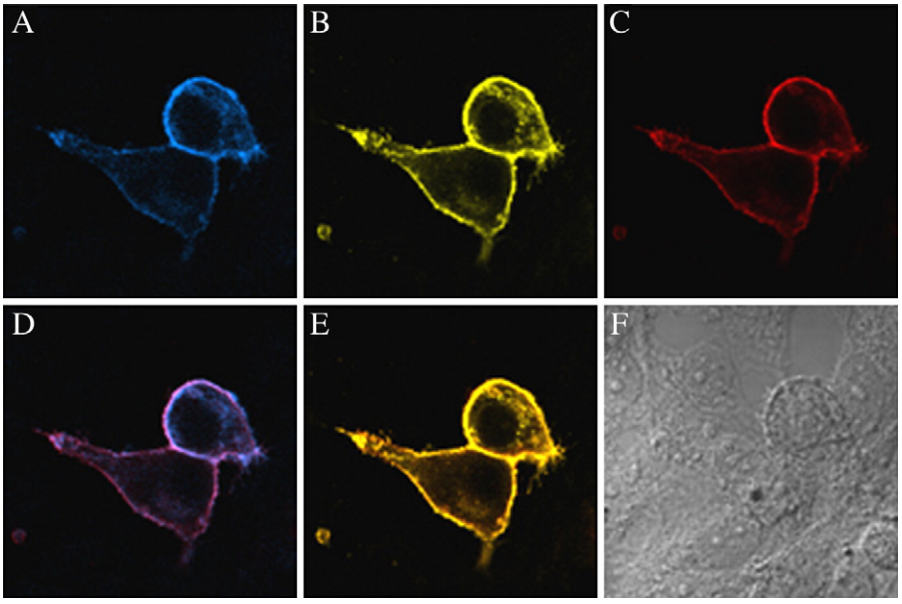

Fig. 3. Cell localization of CFP/YFP tagged CD146 in living cells. Mel888 cells were co-transfected with $CD146_{YFP}$ and $CD146_{CFP}$ constructs. After 48 h culture, the cells were observed under a confocal microscope at the CFP (A) or YFP (B) channel. The CD146 fusion proteins on the cell surface were also recognized by mAb AA98 with cy-chrome (C). (D) and (E) show the merging of AA98/cy-chrome with either CFP or YFP. (F) shows the corresponding phase-contrast images of the cells.

corresponds to the size of CD146 monomer and the 200-kDa corresponds to the size of CD146 dimer. No cross-reaction was detected with a secondary HRP-conjugated anti-rabbit IgG (Fig. 1B, D, F), and also no bands were seen in the immunoprecipitations using mIgG as negative control (data not shown), indicating that the CD146 dimer and monomer were specifically recognized by the two different anti-CD146 antibodies. These results demonstrate that the CD146 dimer and its monomer were both present in all CD146-expressing cells tested, whether they were tumor cell (A375), normal cell (ECV304) or the cells transfected with a CD146 expression plasmid (CD146-positive Mel888). Interestingly, we also observed that the dimer/monomer ratio in melanoma cell line A375 and CD146-positive Mel888 was significantly higher than that in the normal cell line ECV304 (Fig. 1G), implying that dimerization of CD146 may be associated with malignancy.

3.2. Localization of fluorescence-fused CD146 in living cells

In order to study the localization and dimerization of CD146 in living cells, we prepared YFP and CFP-tagged CD146 constructs ($CD146_{YFP}$ and $CD146_{CFP}$) (Fig. 2). The CD146 negative Mel888 cells were pairwise co-transfected with these constructs, and the clones co-expressing $CD146_{YFP}$ and $CD146_{CFP}$ were selected. Expression of CD146 fusion proteins in these doubly transfected cells was detected under a confocal laser scanning microscope. Fig. 3 shows two representative double transfected clones. A high degree of peripheral fluorescence was seen on the cell surface and no fluorescence was detected in either cytosol or nucleus, indicating that the fluorescence-tagged CD146 presented the same cellular localization as its native status. In addition, these images indicated that $CD146_{CFP}$ (Fig. 3A) and $CD146_{YFP}$ (Fig. 3B) were co-expressed within the same population of cells. To further confirm that the yellow and cyan fluorescence on the cell surface represent the YFP- and CFP-tagged CD146, but not YFP and CFP alone, we stained these cells using mAb AA98 combined with cy-chrome dye giving a red fluorescence (Fig. 3C). The confocal images of either CFP or YFP fluorescence merged with AA98 cy-chrome fluorescence (Fig. 3D and E) indicate that the CD146-tagged fusion proteins are co-expressed on cell membrane.

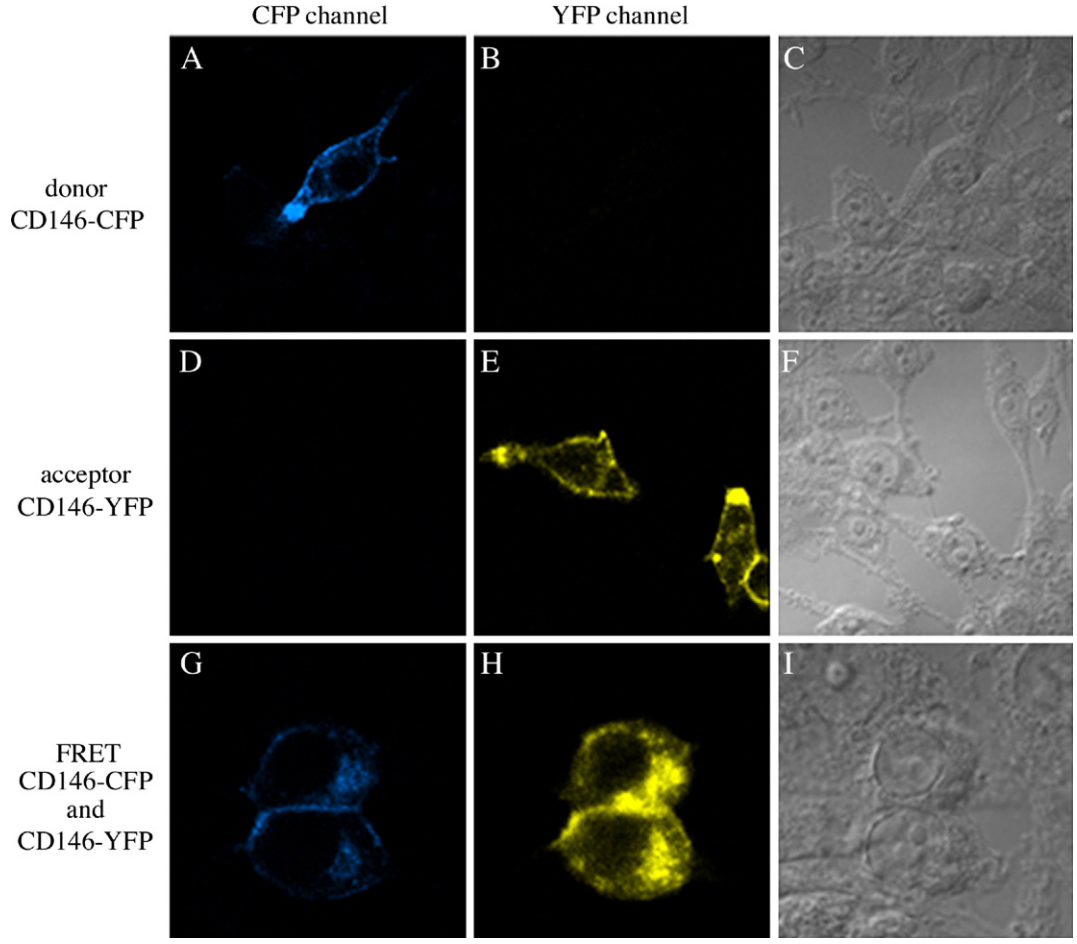

Fig. 4. FRET measurement. The Mel888 cells were transfected with $CD146_{YFP}$ and $CD146_{CFP}$ individually and 48 h later, the cells were visualized under a confocal microscope with optimal filter sets. Cells containing $CD146_{CFP}$ were observed with excitation of CFP and collection CFP image (A), with no crossover with the YFP channel (B). Conversely, in the cells containing $CD146_{YFP}$, YFP was excited and visualized in the YFP image only (E) without crossover with the CFP channel. The cells containing both $CD146_{YFP}$ and $CD146_{CFP}$ were observed at the excitation of the donor (CFP) and collection of both donor (CFP) (G) and acceptor (YFP) emission (H) using the optimal FRET settings. The corresponding phase-contrast images of these cells are presented in (C), (F) and (I).

3.3. FRET imaging CD146 dimerization in living cells

In order to visually monitor the dimerization of CD146 in living cells, FRET measurements were performed using a fluorescence microscope system. We first optimized the filter settings to make sure no crossover excitation of YFP occurred when CFP was excited. For this purpose, we transfected either $CD146_{YFP}$ or $CD146_{CFP}$ into Mel888 cells individually. The results from microscope images are shown in Fig. 4. The $CD146_{CFP}$ alone transfectants showed a cyan fluorescence with excitation at 458 nm and emission at 465–495 nm, and no fluorescence signal was detected in the bandwidth of 565–595 nm ($CD146_{YFP}$ channel) (Fig. 4, panel A and B). Similarly, the cell transfected $CD146_{YFP}$ alone showed a yellow color with excitation at 515 nm and emission at 565–595 nm without crossover to the CFP channel (emission at 465–495 nm) (Fig. 4, panel D and E). At the optimal FRET setting, excitation of $CD146_{CFP}$ (donor) at 458 nm produced a diffuse image of $CD146_{YFP}$ (acceptor) at 565–595 nm, indicating that a transfer of energy was occurred from $CD146_{CFP}$ to $CD146_{YFP}$.

Another measure to ensure the specificity of FRET was acceptor photobleaching. The $CD146_{YFP}$ as acceptor fluorophore was selectively photobleached for 2 min at 515 nm and then the fluorescence intensity of the donor $CD146_{CFP}$ was measured. As shown in Fig. 5, the sharp drop in the fluorescence intensity of the acceptor YFP (Fig. 5A and B) was compensated for by the increase in the intensity of the donor CFP (Fig. 5C and D). This increase was due to the lack of acceptor absorbing the energy liberated by the donor, which in turn leads to a higher emission from the donor. Moreover, we calculated the FRET efficiency as 20.1%. Based on the above observations, we concluded that the FRET signal observed upon co-expression of $CD146_{YFP}$ and $CD146_{CFP}$ resulted from specific dimerization of CD146 in living cells.

3.4. Regulation of CD146 dimerization by A375-CM and mAb AA98

We have previously observed tumor conditional medium induced endothelial cell adhesion and migration. However, these cell activities were inhibited by mAb AA98. To test the molecular organization of CD146 on the cell surface under the influence of extracellular stimulators, we used tumor conditional medium (A375-CM) as stimulator to culture ECV304 cells, and then visualized the CD146 dimer/monomer ratio in the treated cells using immunoprecipitation and Western blotting analysis. The results showed that CD146 dimerization was greatly increased in the endothelial cells after treated with A375-CM. Interestingly, the higher level of CD146 dimerization was dramatically reduced by mAb AA98, regardless of whether CD146 dimerization induced by A375-CM in endothelial cells or naturally existed in melanoma A375 cells (Fig. 6). These results demonstrate that the CD146 dimerization can be up-regulated by A375-CM and down-regulated by mAb AA98.

3.5. CD146 dimerization is associated with the NF-kappa B pathway

It has been shown that many tumors secret several cytokines which trigger signaling and induce NF-kappa B activation, resulting in changes in cell behavior. NF-kappa B is

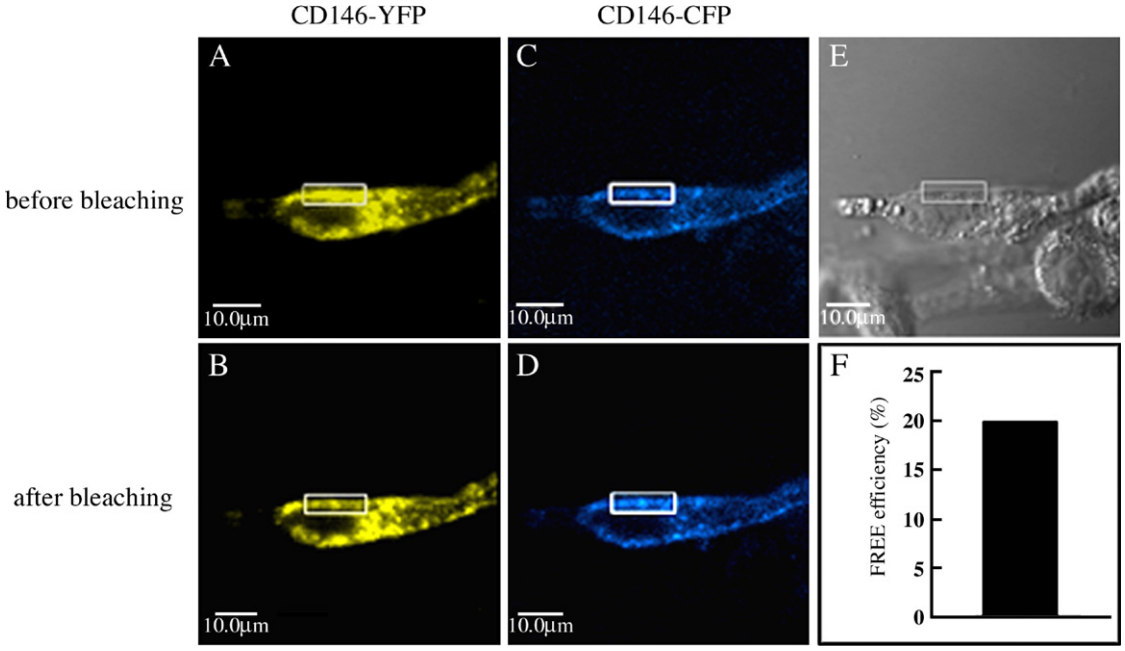

Fig. 5. Acceptor photobleaching. In $CD146_{YFP}$ and $CD146_{CFP}$ constructs transfected Mel888 cells, the acceptor (YFP) was photobleached by repeated scanning with the 515-nm laser. (A) and (B) present pre- and post-bleached images of the acceptor. (C) and (D) are corresponding donor (CFP) images in the same cell. (E) shows the corresponding phase-contrast images of the cell. (F) Quantification of FRET efficiency (E, %) using the acceptor photobleaching method. The FRET efficiency was 20.1%.

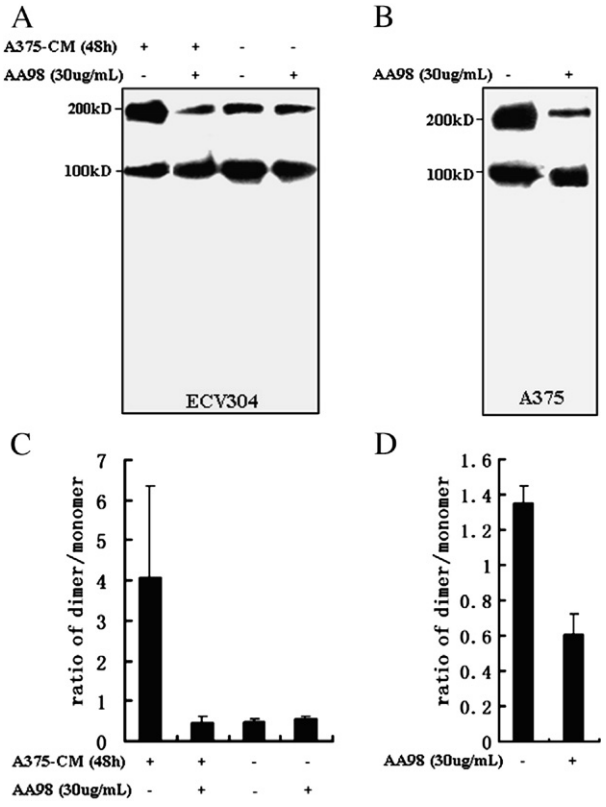

Fig. 6. CD146 dimerization is enhanced by A375-CM but suppressed by mAb AA98. (A) ECV304 cells were treated with or without AA98 and A375-CM, and with only one of each. (B) A375 cells were treated with or without mAb AA98. The cell lysates were immunoprecipitated with monoclonal anti-CD146 antibody, AA98, followed by Western blotting with rabbit anti-CD146 antibody. The ratio of the CD146 dimer and monomer were qualified by densitometry using the data from three independent experiments (C and D).

an inducible transcription factor that belongs to the Rel family. In its resting state, NF-kappa B complexed with IκBα exists in cytoplasm. When a cell receives certain extracellular signals, IκBα is rapidly phosphorylated and degraded via the ubiquitin-proteasome pathway, and NF-kappa B is redistributed from the cytosol into the nucleus, regulating the expression of many genes. Based on previous studies, we wondered whether the A375-CM enhanced CD146 dimerization might be associated with NF-kappa B activation. To test this, we analyzed the NF-kappa B nuclear translocation in ECV304 cells after A375-CM treatment. The fluorescence microscope images using anti-NF-kappa B antibody combined with FITC are shown in Fig. 7A. We found that NF-kappa B was presented in the cytosol of ECV304 cells when cultured in normal DMEM medium. After stimulation with A375-CM, the NF-kappa B was redistributed from the cytosol into the nuclei. However, an NF-kappa B inhibitor, BAY11-7082, suppressed the nuclear translocation of NF-kappa B which was induced by A375-CM.

These observations were further confirmed using Western blotting analysis as shown in Fig. 7B. In ECV304 cells grown in normal medium, most IκB was found in the cytosol fraction and very little NF-kappa B was found in the nuclear fraction. However, after stimulation with A375-CM, the NF-kappa B in the nuclear fraction was dramatically increased and IκB in the cytosol fraction was decreased. Similarly, as seen in Fig. 7A, the amount of NF-kappa B in the nuclear fraction was reduced by an NF-kappa B inhibitor. These observations indicate that NF-kappa B activation in endothelial cells is regulated by tumor conditional medium from A375 cells.

Interestingly, we found that the NF-kappa B activation was associated with CD146 dimerization. As shown in Fig. 7C, the majority of CD146 is in the monomeric form in normal ECV304 cells. After treatment with A375-CM, the dimer/monomer ratio in ECV304 cells was significantly increased. However, this increased CD146 dimerization could be suppressed by the NF-kappa B inhibitor, BAY 11-7802. Whereas the BAY 11-7802 did not dissociate the CD146 dimer existed in the ECV304 without A375-CM treatment (data no shown). This suggests that CD146 dimerization is triggered by A375-CM and regulated through the NF-kappa B pathway.

4. Discussion

In this study, we provided the first evidence that CD146 dimerization occurs in living cells by demonstrating that (1) the CD146 dimer (200 kDa) was specifically pulled-down with mAb AA98, and recognized by anti-CD146 rabbit antibody, (2) A specific FRET signal was observed in living cells which were co-expressing CFP/YFP-tagged CD146, indicating CD146 homophilic interaction. This observation confirms the occurrence of CD146 dimerization in living cells.

Another important finding in this study is that CD146 dimerization was regulated by anti-CD146 mAb AA98 and A375-CM through the NF-kappa B pathway. However, the molecular organization of CD146 in the presence of stimulator or inhibitor remained unclear. Here, we provided several lines of evidence to support the hypothesis that CD146 dimerization is regulated by mAb AA98 and A375-CM through the NF-kappa B pathway. First, we found that the dimer and monomer of CD146 both existed in the cells tested and the dimer/monomer ratio in tumor cells (A375) was significantly higher than that in normal endothelium. Second, CD146 dimerization in endothelial cells was up-regulated by A375-CM. After culture of the endothelial cells in A375-CM for 2 days, the amount of the dimeric form of CD146 was greatly enhanced. In contrast, we found that mAb AA98 inhibited the dimerization of CD146 in melanoma A375 cells. These results strongly suggest that CD146 dimerization is a dynamic process in living cells and responds to the stimuli in the tumor microenvironment and to inhibitors like mAb AA98. Finally, A375-CM-induced CD146 dimerization could be reduced by an NF-kappa B inhibitor BAY 11-7082, indicating that CD146 dimerization up-regulation by A375-CM is through the NF-kappa B pathway.

Many factors in tumor conditional medium, such as TNF-α, can activate the NF-kappa B pathway, inducing the expression of many genes involved in tumor progression. Our previous studies have demonstrated that tumor conditional medium up-regulated the CD146 expression and induced the migration and

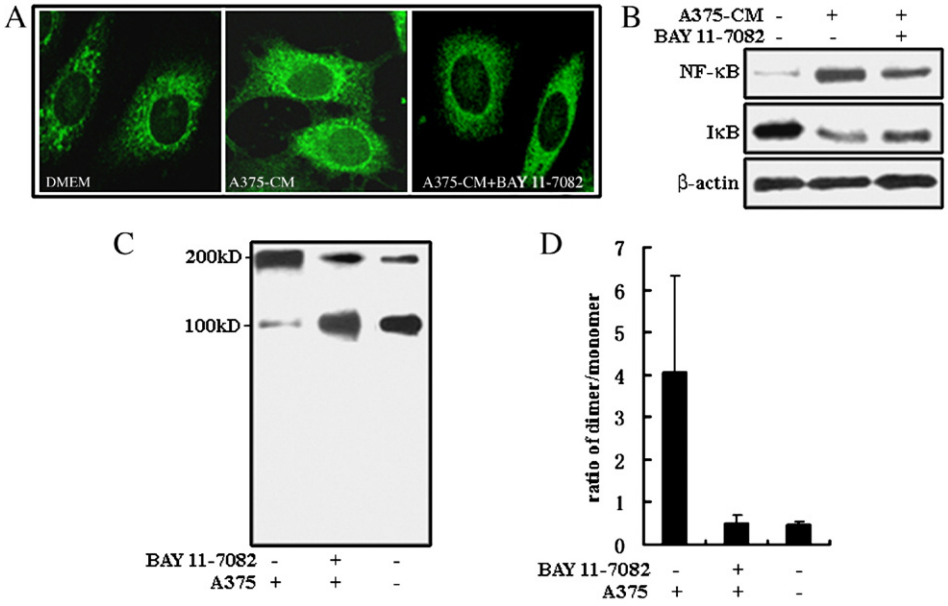

Fig. 7. CD146 dimerization is associated with NF-kappa B pathway. (A) Immunofluorescence of the ECV304 cells stained with anti-p65 antibody and observed under a confocal laser scanning microscope. NF-kappa B translocation was induced by A375-CM and suppressed by the NF-kappa B inhibitor, BAY 11-7082. No NF-kappa B nuclear translocation was detected in the ECV304 cultured in DMEM medium. This observation was confirmed by Western blotting (B). The NF-kappa B in the nuclear extracts was detected by anti-p65 antibody, whereas the IκB and β-actin as control in the cytosol extracts were detected by anti-IκB and anti-β-actin antibody. (C) The immunoprecipitations with monoclonal anti-CD146 antibody, AA98 were stained using rabbit anti-CD146 antibody. Western blotting showed that the CD146 dimerization in the ECV304 cells was enhanced by A375-CM and suppressed by the NF-kappa B inhibitor, BAY 11-7082. (D) The ratio of the CD146 dimer and monomer were qualified by densitometry using the data from three independent experiments.

angiogenesis of endothelial cells, whereas these cell activities were suppressed by mAb AA98 via inhibition of NF-kappa B [8,20]. Here we found that A375 conditional medium induced the CD146 dimerization though the NF-kappa B pathway. And the mAb AA98 and NF-kappa B inhibitor both dissociated CD146 dimerization. Based on these observations, we hypothesize that mAb AA98 inhibits NF-kappa B translocation via its suppression of CD146 dimerization. However, it is still not clear which is the first event, CD146 dimerization or NF-kappa B activation, inhibited by mAb AA98. Another explanation might be that certain factors in A375 conditional medium activate NF-kappa B, resulting in the expression of many genes, possibly including the ligand of CD146. As a result, the increased amount of ligand may engage with the CD146 molecule and further induce its dimerization. Like many other membrane receptors [21], CD146 dimerization may initiate signaling transduction since the CD146 molecule possesses potential recognition sites for protein kinases in its cytoplasmic domain. The inhibitory effect of mAb AA98 on CD146 dimerization might be due to blocking interaction between CD146 and its ligand. Although the ligand of CD146 has not been identified, there is evidence that many melanoma cells express the CD146 ligand [22], and CD146 mediated cell–cell adhesion through its unidentified ligand may represent an important role in cell biological function, and perhaps in tumor growth and metastasis. It will be of interest to identify the CD146 ligand and better understand the role of CD146 in signaling.

In summary, this study provides the first evidence that CD146 dimerization occurs in living cells and is regulated by the tumor microenvironment through the NF-kappa B pathway. The dynamic nature of CD146 dimerization may be associated with tumor malignancy.

Acknowledgements

We thank Dr. J. Johnson for supplying the CD146-transfected Mel 888 cells, the parental Mel 888 cells and CD146 gene contained in pUC-CD146 plasmids. We also thank Dr. Sarah Perrett for helpful suggestions and critical reading of the manuscript. This work was supported by the National 863 grant, the National Natural Sciences Foundation, a Chinese Academy of Sciences grant and the Program of Founding Research Centers for Emerging and Reemerging Infectious Diseases by the Ministry of Education, Culture, Sports, Science and Technology (MEXT) of Japan.

References

[1] C.L. Holness, D.L. Simmons, Structural motifs for recognition and adhesion in members of the immunoglobulin superfamily, J. Cell Sci. 107 (1994) 2065–2070.
[2] J.P. Johnson, U. Rothbacher, C. Sers, The progression associated antigen MUC18: a unique member of the immunoglobulin supergene family, Melanoma Res. 3 (1993) 337–340.
[3] J.M. Lehmann, G. Riethmuller, J.P. Johnson, MUC18, a marker of tumor progression in human melanoma, shows sequence similarity to the neural cell adhesion molecules of the immunoglobulin superfamily, Proc. Natl. Acad. Sci. U. S. A. 86 (1989) 9891–9895.
[4] J.M. Lehmann, B. Holzmann, E.W. Breitbart, P. Schmiegelow, G. Riethmuller, J.P. Johnson, Discrimination between benign and malignant cells of melanocytic lineage by two novel antigens, a glycoprotein with a

molecular weight of 113 000 and a protein with a molecular weight of 76 000, Cancer Res. 47 (1987) 841–845.
[5] S. Xie, M. Luca, S. Huang, M. Gutman, R. Reich, J.P. Johnson, M. Bar-Eli, Expression of MCAM/MUC18 by human melanoma cells leads to increased tumor growth and metastasis, Cancer Res. 57 (1997) 2295–2303.
[6] K. Satyamoorthy, J. Muyrers, F. Meier, D. Patel, M. Herlyn, Mel-CAM-specific genetic suppressor elements inhibit melanoma growth and invasion through loss of gap junctional communication, Oncogene 20 (2001) 4676–4684.
[7] L. Mills, C. Tellez, S. Huang, C. Baker, M. McCarty, L. Green, J.M. Gudas, X. Feng, M. Bar-Eli, Fully human antibodies to MCAM/MUC18 inhibit tumor growth and metastasis of human melanoma, Cancer Res. 62 (2002) 5106–5114.
[8] X. Yan, Y. Lin, D. Yang, Y. Shen, M. Yuan, Z. Zhang, P. Li, H. Xia, L. Li, D. Luo, Q. Liu, K. Mann, B.L. Bader, A novel anti-CD146 monoclonal antibody, AA98, inhibits angiogenesis and tumor growth, Blood 102 (2003) 184–191.
[9] C.B. St, C. Rago, V. Velculescu, G. Traverso, K.E. Romans, E. Montgomery, A. Lal, G.J. Riggins, C. Lengauer, B. Vogelstein, K.W. Kinzler, Genes expressed in human tumor endothelium, Science 289 (2000) 1197–1202.
[10] N. Bardin, F. Anfosso, J.M. Masse, E. Cramer, F. Sabatier, B.A. Le, J. Sampol, F. gnat-George, Identification of CD146 as a component of the endothelial junction involved in the control of cell–cell cohesion, Blood 98 (2001) 3677–3684.
[11] B. Chan, S. Sinha, D. Cho, R. Ramchandran, V.P. Sukhatme, Critical roles of CD146 in zebrafish vascular development, Dev. Dyn. 232 (2005) 232–244.
[12] Q. Liu, X. Yan, Y. Li, Y. Zhang, X. Zhao, Y. Shen, Pre-eclampsia is associated with the failure of melanoma cell adhesion molecule (MCAM/CD146) expression by intermediate trophoblast, Lab. Invest. 84 (2004) 221–228.
[13] I.M. Shih, R.J. Kurman, Expression of melanoma cell adhesion molecule in intermediate trophoblast, Lab. Invest. 75 (1996) 377–388.
[14] Q. Liu, X. Zhao, Y. Zhang, Y. Shen, Y. Liu, X. Yan, Melanoma cell adhesion molecule (MCAM/CD146) is a critical molecule in trophoblast invasion, Prog. Biochem. Biophys. 34 (2004) 309–312.
[15] A.N. Solovey, L. Gui, L. Chang, J. Enenstein, P.V. Browne, R.P. Hebbel, Identification and functional assessment of endothelial P1H12, J. Lab. Clin. Med. 138 (2001) 322–331.
[16] F. Anfosso, N. Bardin, V. Frances, E. Vivier, L. Camoin-Jau, J. Sampol, F. gnat-George, Activation of human endothelial cells via S-endo-1 antigen (CD146) stimulates the tyrosine phosphorylation of focal adhesion kinase p125 (FAK), J. Biol. Chem. 273 (1998) 26852–26856.
[17] I. Hunter, H. Sawa, M. Edlund, B. Obrink, Evidence for regulated dimerization of cell–cell adhesion molecule (C-CAM) in epithelial cells, Biochem. J. 320 (1996) 847–853.
[18] T. Zhao, P.J. Newman, Integrin activation by regulated dimerization and oligomerization of platelet endothelial cell adhesion molecule (PECAM)-1 from within the cell, J. Cell Biol. 152 (2001) 65–73.
[19] M. Vicente-Manzanares, M. Rey, D.R. Jones, D. Sancho, M. Mellado, J.M. Rodriguez-Frade, M.A. del Pozo, M. Yanez-Mo, A.M. de Ana, A. Martinez, I. Merida, F. Sanchez-Madrid, Involvement of phosphatidylinositol 3-kinase in stromal cell-derived factor-1 alpha-induced lymphocyte polarization and chemotaxis, J. Immunol. 163 (1999) 4001–4012.
[20] P. Bu, L. Gao, J. Zhuang, J. Feng, D. Yang, X. Yan, Anti-CD146 monoclonal antibody AA98 inhibits angiogenesis via suppression of nuclear factor-kappaB activation, Mol. Cancer Ther. 5 (2006) 2872–2878.
[21] S. Bishayee, S. Majumdar, J. Khire, M. Das, Ligand-induced dimerization of the platelet-derived growth factor receptor. Monomer-dimer interconversion occurs independent of receptor phosphorylation, J. Biol. Chem. 264 (1989) 11699–11705.
[22] I.M. Shih, D. Speicher, M.Y. Hsu, E. Levine, M. Herlyn, Melanoma cell–cell interactions are mediated through heterophilic Mel-CAM/ligand adhesion, Cancer Res. 57 (1997) 3835–3840.